FAM65B is a membrane-associated protein of hair cell stereocilia required for hearing

Oscar Diaz-Horta[a,b,1], Asli Subasioglu-Uzak[a,b,c,1], M'hamed Grati[d], Alexandra DeSmidt[e], Joseph Foster II[a,b], Lei Cao[a,b], Guney Bademci[a,b], Suna Tokgoz-Yilmaz[f], Duygu Duman[f], F. Basak Cengiz[f], Clemer Abad[a,b], Rahul Mittal[d], Susan Blanton[a,b], Xue Z. Liu[d], Amjad Farooq[g], Katherina Walz[a,b], Zhongmin Lu[e], and Mustafa Tekin[a,b,f,2]

[a]Dr. John T. Macdonald Foundation Department of Human Genetics, [b]John P. Hussman Institute for Human Genomics, and Departments of [d]Otolaryngology and [g]Biochemistry and Molecular Biology, University of Miami Miller School of Medicine, Miami, FL 33136; [c]Department of Medical Genetics, Erciyes University School of Medicine, Kayseri 38039, Turkey; [e]Department of Biology, University of Miami, Miami, FL 33146; and [f]Division of Pediatric Genetics, Ankara University School of Medicine, Ankara 06100, Turkey

Edited by Stephen T. Warren, Emory University School of Medicine, Atlanta, GA, and approved June 4, 2014 (received for review January 31, 2014)

In a large consanguineous Turkish kindred with recessive nonsyndromic, prelingual, profound hearing loss, we identified in the gene *FAM65B* (MIM611410) a splice site mutation (c.102-1G>A) that perfectly cosegregates with the phenotype in the family. The mutation leads to exon skipping and deletion of 52-amino acid residues of a PX membrane localization domain. FAM65B is known to be involved in myotube formation and in regulation of cell adhesion, polarization, and migration. We show that wild-type *Fam65b* is expressed during embryonic and postnatal development stages in murine cochlea, and that the protein localizes to the plasma membranes of the stereocilia of inner and outer hair cells of the inner ear. The wild-type protein targets the plasma membrane, whereas the mutant protein accumulates in cytoplasmic inclusion bodies and does not reach the membrane. In zebrafish, knockdown of *fam65b* leads to significant reduction of numbers of saccular hair cells and neuromasts and to hearing loss. We conclude that FAM65B is a plasma membrane-associated protein of hair cell stereocilia that is essential for hearing.

deafness | whole-exome sequencing | congenital | Mendelian disorder | sensorineural

Hearing loss is the most common sensory problem, affecting approximately 1 in 500 newborns. Most cases are the consequence of mutations in single genes with specific functions in the inner ear (1) (http://hereditaryhearingloss.org). Hearing depends on the ability of the inner ear to convert acoustic waves into electrical signals. This process originates in the stereocilia, actin-rich structures that project from the apical pole of cochlear hair cells and are interconnected in the shape of a staircase to form the hair bundle. Most of the ∼50 hair-bundle proteins identified so far are the products of genes that when mutated lead to hearing loss (2). Thus, the genetic approach has played a major role in elucidating the molecular components of normal hearing.

Here we present Family With Sequence Similarity 65, Member B (FAM65B, MIM611410) as a previously unrecognized, plasma membrane-associated protein of hair cell stereocilia. The critical role of FAM65B in human hearing was revealed by genetic analysis of a large family with hereditary deafness. In the zebrafish, knocking down the ortholog of *FAM65B* led to sensorineural hearing loss.

Results

A Splice Site Mutation in *FAM65B* Causes Profound Sensorineural Hearing Loss in a Turkish Family. In a large consanguineous kindred of Turkish origin (Fig. 1*A*), six affected individuals had symmetric profound sensorineural hearing loss (Fig. 1*B*). Anamnestic evaluation and audiograms indicated congenital/prelingual onset hearing loss in all affected individuals. Available audiograms do not suggest progression of hearing loss. Transient evoked otoacoustic emissions and acoustic reflexes were negative in all affected members of the family. Auditory brainstem responses were absent as well. Affected individuals had neither delay in gross motor development nor balance problems, vertigo, dizziness, or nystagmus. Tandem walking was normal and Romberg test was negative. High-resolution computerized tomography scans of the temporal bone in two affected members (IV:5 and IV:6) were normal. Other examinations, including anterior chamber and fundus of the eyes, ECGs, liver enzymes, kidney function, serum electrolytes, urinalysis, and complete blood counts, were normal in all affected members of the studied family.

Sequencing of the whole exome in individual IV:6 generated a mean coverage of 52-fold; 92.5% of targeted reads had >2-fold coverage. DNA variants were filtered for frequency [minor allele frequency <0.005 in dbSNP137 (http://www.ncbi.nlm.nih.gov/projects/SNP) and National Heart, Lung, and Blood Institute cohorts (http://evs.gs.washington.edu/EVS) and the University of Miami internal exome database] and then classified by predicted function: nonsense mutations, frame-shift mutations, variants within 1 bp of a splice site, and putatively damaging missense variants [defined as predicted to be damaging by the PolyPhen-2 or SIFT online tools (*SI Materials and Methods*) and the variant allele present in at most one other sequenced species]. Given that the family showed autosomal recessive inheritance, we identified all homozygous or compound heterozygous variants meeting these criteria. Only one variant did so: Individual IV:6 was homozygous for chr6:24,874,028G>A (hg19), corresponding to *FAM65B* c.102-1G >A (NM_014722.2, GenBank) at the *FAM65B* intron 2 acceptor splice site.

Significance

Concerted action of thousands of proteins is required for the inner ear to convert acoustic waves into electrical signals for hearing. Many of these proteins are currently unknown. This study uses a genetic approach to identify *FAM65B* as a gene mutated in a family with sensorineural hearing loss. Characterization of FAM65B shows that it is a component of the plasma membrane of the stereocilia hair bundle, the essential organelle in which electrical signals originate in the inner ear. Thus, FAM65B is a previously unrecognized component of the inner ear that is crucial for hearing.

Author contributions: O.D.-H., A.S.-U., M.G., and M.T. designed research; O.D.-H., A.S.-U., M.G., A.D., J.F., L.C., G.B., S.T.-Y., D.D., F.B.C., C.A., R.M., A.F., and Z.L. performed research; O.D.-H., A.S.-U., M.G., S.B., X.Z.L., A.F., K.W., Z.L., and M.T. analyzed data; and O.D.-H., A.S.-U., M.G., A.F., Z.L., and M.T. wrote the paper.

The authors declare no conflict of interest.

This article is a PNAS Direct Submission.

[1]O.D.-H. and A.S.-U. contributed equally to this work.

[2]To whom correspondence should be addressed. E-mail: mtekin@med.miami.edu.

This article contains supporting information online at www.pnas.org/lookup/suppl/doi:10.1073/pnas.1401950111/-/DCSupplemental.

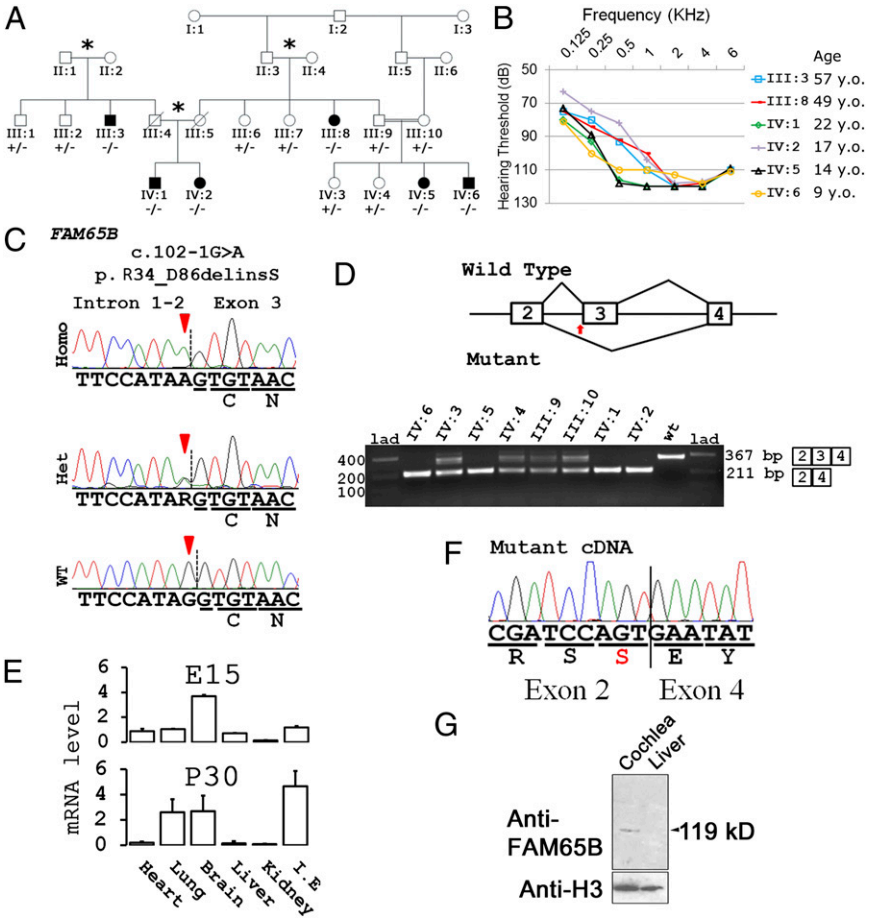

Fig. 1. Gene discovery. (*A*) Family of Turkish origin with prelingual hearing loss (black symbols) and genotypes at *FAM65B* c.102-1G>A. The double bars indicate a consanguineous marriage, and asterisks indicate marriages of persons from the same village. $^{-/-}$, homozygous mutant; $^{+/-}$, heterozygous mutant; $^{+/+}$, homozygous wild-type individuals. (*B*) Audiograms showing profound sensorineural hearing loss in affected individuals. (*C*) Genomic sequence at *FAM65B* c.102-1G>A. (*D*) Schematics showing splicing of WT and mutant mRNA variants. Amplified cDNA from homozygous and heterozygous individuals show shorter length (lower panel). (*F*) Nucleotide sequence of amplicons from homozygous individuals proving skipping of *FAM65B* exon 3 as a result of the mutation. (*E*) Expression levels of *Fam65b* transcript in different mouse tissues at embryonic day (E)15 and postnatal day (P)30. I.E, inner ear. Error bars represent the standard error of the mean of 3 independent experiments. (*G*) Western blots of protein extracts from the inner ear and liver of adult mice. Arrowheads in *C* and the arrow in *D* indicate the location of the splice site variation.

In individual IV:6, this variant was within a 28.8-Mb region of homozygosity between chr6:3,155,072 and chr6:31,938,736. Sanger sequencing of 13 other informative family members for the variant showed cosegregation with the phenotype in the family (Fig. 1 *A* and *C*). The variant was absent from public databases of sequenced individuals and also absent from 330 Turkish controls. Gel electrophoresis and sequence analysis of cDNA synthesized from leukocyte mRNA from family members

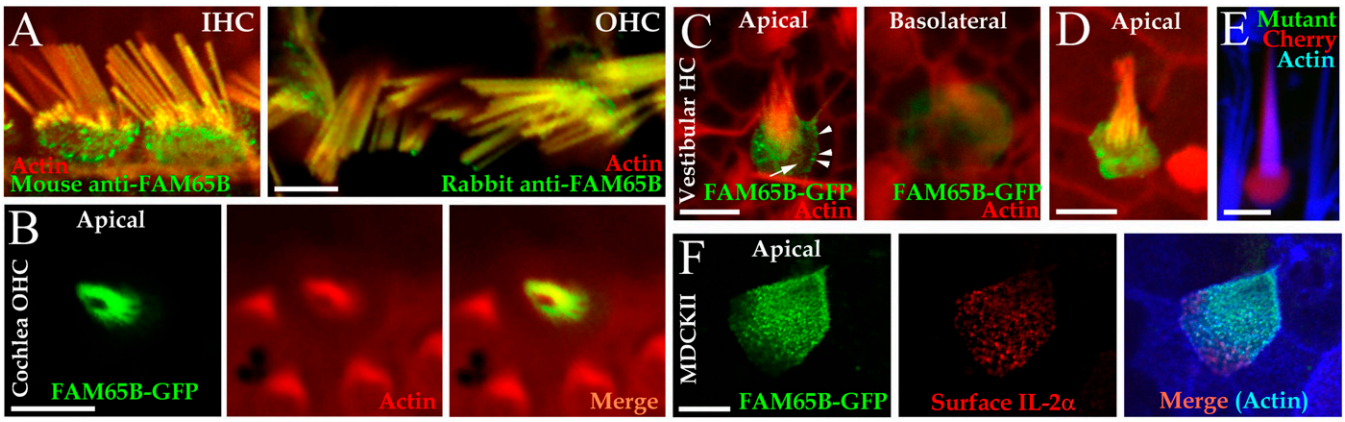

Fig. 2. Localization of Fam65b to the plasma membrane of hair cell stereocilia. (*A*) Confocal scans of 4-wk-old rat organ of Corti inner hair cells (IHCs) and outer hair cells (OHCs) showing Fam65b in the apical region of the hair cells including stereocilia. For immunostaining, two different antibodies raised against different FAM65B epitopes were used. (*B–D*) Confocal scans of wild-type FAM65B (green) in organotypic rat cochlea OHCs (*B*) and in vestibular hair cells with moderate (*C*) and high (*D*) expression levels. Actin is counterstained in red. In *C*, arrowheads indicate green fluorescent clusters representing fusion-exocytosis vesicles in the pericuticular area. The arrow indicates localization of FAM65B-GFP in supracuticular plasma membrane. (*E*) Coexpression of mutant FAM65B-GFP and Cherry (red) in hair cells showing the absence of GFP signals corresponding to the mutant FAM65B-GFP protein in vestibular hair cell stereocilia. The Cherry reporter is present in hair cytosol and within the stereocilia counterstained for actin (blue). (*F*) Colocalization of FAM65B-GFP (green) and plasma membrane marker IL-2α receptor (red) in polarized MDCK II cells at the microvillar plasma membrane of the apical cell surface; actin is visualized in blue. (Scale bars, 5 μm.)

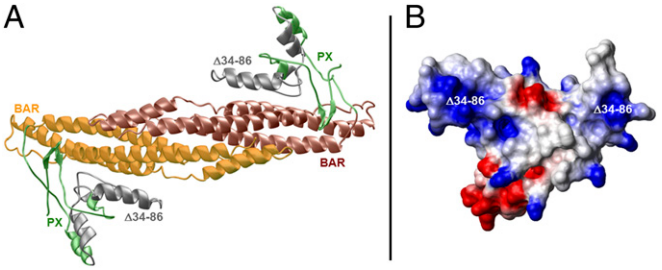

Fig. 3. Structure of the PX–BAR module of human FAM65B. (*A*) Ribbon representation of the structural model of the predicted PX–BAR module, responsible for targeting and binding the protein to the cell membrane. The PX domain promotes membrane localization by binding to phospholipids. Together, the nexin PX and BAR domains both aid protein sorting and act as sensors of membrane curvature. The PX–BAR module is shown as a homodimer, with the N-terminal PX domain (residues 1–110) colored green and gray and the more C-terminal BAR domain (residues 111–300) colored yellow and brown. The region harboring the deletion of residues 34–86 (Δ34–86) is colored gray and maps to the core region of the PX domain, critical for its membrane localization. (*B*) Electrostatic surface potential map of the monomeric PX domain derived from the structural model of the PX–BAR dimeric module. Blue and red colors denote the density of positive and negative charges, respectively, whereas the apolar and polar surfaces are indicated by white and gray, respectively. The Δ34–86 deletion maps to the region within the PX domain harboring predominantly a net positive charge (colored blue).

revealed that exon 3 of *FAM65B* was absent in all affected relatives, whereas heterozygous individuals (III:9, III:10, IV:3, IV:4) carried both the wild-type and the mutant transcripts (Fig. 1 *D* and *F*). Thus, the mutation causes an in-frame skipping of exon 3, comprising amino acid residues 34–86 (p.R34_D86delinsS, NP_055537.2, GenBank; Δ34–86). Of 248 other autosomal recessive families or 437 simplex cases with nonsyndromic hearing loss, no others harbored mutations in *FAM65B*.

Fam65B Is Present in Apical Plasma Membrane of Mammalian Hair Cells. Mouse *Fam65b* and human *FAM65B* have 86% identical transcripts and 87% identical proteins. Reverse transcription followed by quantitative PCR (RT-qPCR) of RNA from mouse tissues showed that *Fam65b* is widely expressed (Fig. 1*E*). The highest levels of expression were found in the embryonic brain followed by the inner ear and the postnatal inner ear. The specificity of RT-qPCR amplicons was verified by Sanger sequencing. Western blot analysis showed a band of ∼119 kDa in protein extracted from adult mouse cochlea, the predicted size of Fam65b isoform 1 (Fig. 1*G*).

Confocal images of whole-mount immunofluorescence preparations of cochlea neuroepithelium from 4-wk-old rats showed that Fam65b protein was present in the apical stereocilia of inner and outer hair cells (Fig. 2*A*). In hair cells, a tight junctional belt separates the apical domain of the plasma membrane from the basolateral domain and prevents the diffusion of membrane proteins from one domain to the other (3). The cuticular plate of hair cells in the apical cytoplasm precludes the passage of endocytotic and exocytotic vesicles to and from a major portion of the apical membrane. Confocal microscopy of transfected rat cochlear and vestibular explant hair cells showed that wild-type FAM65B-GFP is targeted to the apical plasma membrane compartments of hair cells (apical scans in Fig. 2 *B–D*). The protein was abundant at the vesicular trafficking area of the apical plasma membrane, the region between the cuticular plate and the apical junctional belt (4), showing vesicle-like structures (arrowheads in Fig. 2*C*) in the supracuticular transition zone (arrow in Fig. 2*C*) and in the stereociliar plasma membrane. This profile is very similar to that of calcium-ATPase2, previously shown to localize at the plasma membrane of stereocilia (5). Mutations in the gene encoding for this transporter cause deafness in mice (6), and have been reported to be a genetic modifier of hearing loss in humans (7). Confocal scans of the basolateral poles of transfected hair cells revealed FAM65B-GFP in cytosol but not in plasma membrane, suggesting that it is in intracellular membrane trafficking compartments (Fig. 2*C*, basolateral). To confirm the membrane localization of FAMB65, polarized Madin–Darby canine kidney (MDCK) II cells were doubly transfected with constructs encoding FAM65B-GFP and plasma membrane marker IL-2α receptor. Immunocytochemistry shows colocalization of FAM65B-GFP with the IL-2α receptor subunit in the apical plasma membrane (Fig. 2*E*).

Δ34–86 Impairs FAM65B Subcellular Distribution. The N-terminal region of FAM65B (residues 1–300) shares sequence similarity with PX–BAR modules (8, 9). This protein module is present in the sorting nexins, which play a key role in targeting of cargos to and from the plasma membrane (10–13). The PX domain

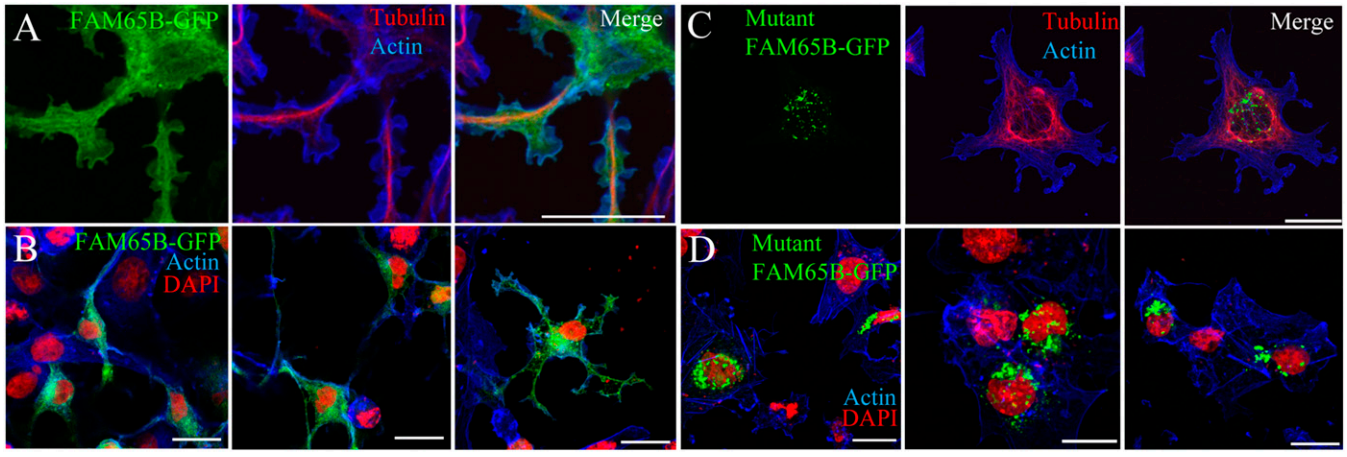

Fig. 4. Effect of the FAM65B Δ34–86 mutation on subcellular localization. (*A* and *B*) In transfected COS7 cells, the green fluorescence corresponding to wild-type FAM65B-GFP defines the plasma membrane of the cell as the cortical actin network does (in blue) and is also present in the intracellular membrane compartment (*A*, higher magnification; *B*, overview of cell groups). (*C* and *D*) Localization of mutant FAM65B-GFP to cytoplasmic inclusion bodies and not to membranes (*D*, overview of cell groups). The microtubule network of the cell cytoskeleton is visualized using an antibody against β-tubulin (*A* and *D*), whereas the cellular nuclei are stained with DAPI. (Scale bars, 10 μm.)

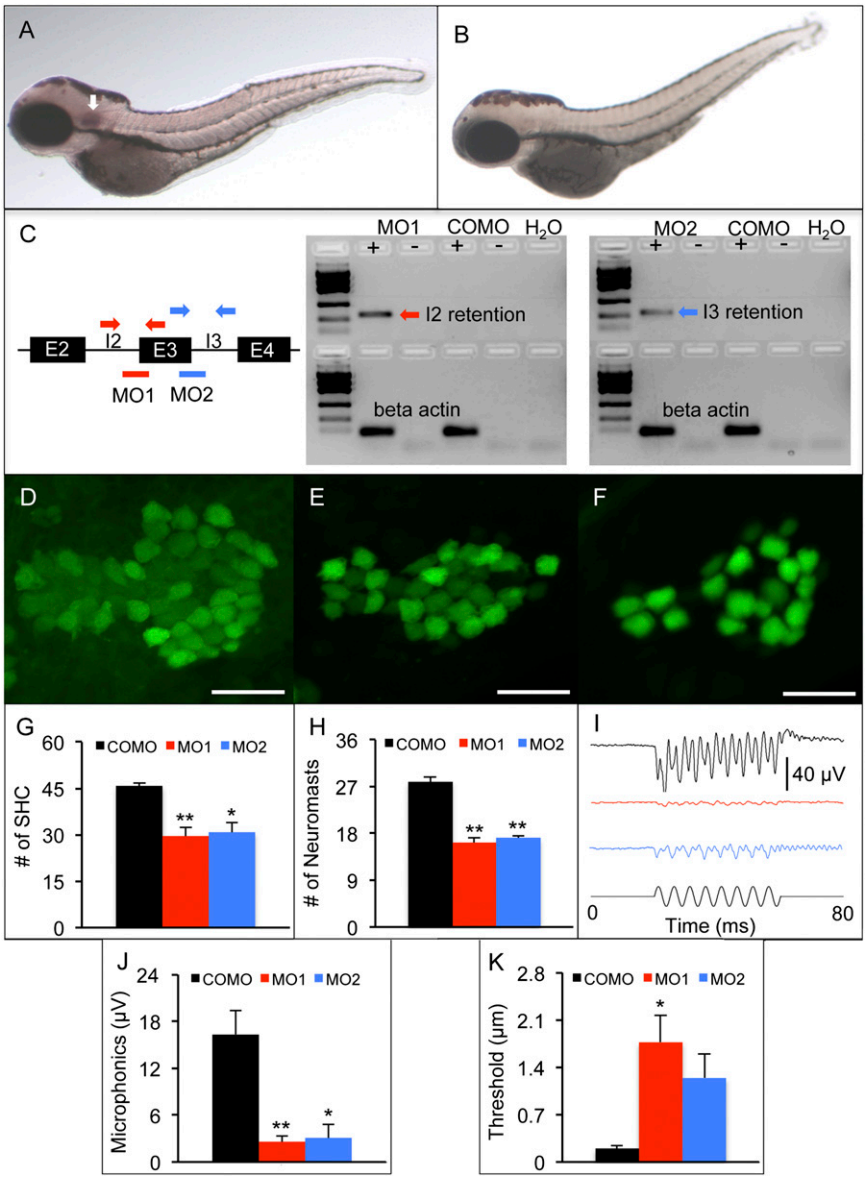

Fig. 5. Zebrafish model of *fam65b* sensorineural hearing loss. (*A* and *B*) In situ hybridization whole mounts of 3 days postfertilization (dpf), wild-type AB zebrafish with *fam65b* antisense probe (*A*) and sense probe (*B*). The arrow in *A* indicates *fam65b* expression in the otic vesicle. (*C*) (*Left*) A schematic drawing of morpholinos (red and blue lines) and primer binding sites (red and blue arrows) used for detection of intron 2 and 3 retention, respectively. (*Center* and *Right*) RT-PCR signals indicating intron retention in MO1 and MO2 morphants but not in control morphants (COMOs). (*D–F*) Confocal images of saccular hair cells (green) of a control morphant (*D*) and MO1 (*E*) and MO2 (*F*) morphants. (Scale bars, 20 μm.) (*G*) Comparison of numbers of saccular hair cells (SHC) among controls ($n = 9$) and MO1 ($n = 7$) and MO2 ($n = 7$) morphants. (*H*) Comparison of numbers of neuromasts per side among controls ($n = 10$) and MO1 ($n = 8$) and MO2 ($n = 17$) morphants. (*I*) Microphonic potential waveforms of control (*Upper* trace) and MO1 and MO2 morphants (two *Middle* traces) in response to 200-Hz sinusoidal stimuli (*Lower* trace) at 5.8-μm displacement. (*J*) Comparison of microphonic amplitude (root mean square) among controls ($n = 7$) and MO1 ($n = 7$) and MO2 ($n = 8$) morphants. Stimuli: 200 Hz at 5.8-μm displacement. (*K*) Comparison of microphonic thresholds among controls ($n = 7$) and MO1 ($n = 7$) and MO2 ($n = 8$) morphants. ANOVAs followed by Tukey posttests were performed to determine the significance of differences. Data are represented as means ± SEM. $^{**}P < 0.001$, $^{*}P < 0.005$.

typically promotes membrane localization of sorting nexins by binding to phospholipids (8, 14, 15). Dimerization potential of the BAR domain mediates heteroassociation between nexins (9, 16, 17). Together, the nexin PX and BAR domains both aid protein sorting and act as sensors of membrane curvature. Analysis of the structure of the N-terminal region of FAM65B, spanning residues 1–300, suggests hallmarks of a canonical PX–BAR module (Fig. 3*A*). The BAR domain of FAM65B appears to drive association of the PX–BAR module into an arc-like homodimer that is presumably important for its ability to sense membrane curvature, and the PX domain acts as an outward protrusion suited for binding to potential membrane phospholipids. The 34- to 86-amino acid segment maps to the core region of the PX domain. Its deletion most likely results in the total collapse of the PX domain structure, thereby altering folding and membrane phospholipid association of FAM65B. This notion is further supported by the fact that the PX domain harboring the residues deleted in the mutation predominantly harbors a net positive surface charge (Fig. 3*B*), which is optimally suited for the recognition of membrane phospholipids.

These predictions were verified experimentally. Confocal microscopy of COS7 cells transfected with construct encoding wild-

type FAM65B-GFP showed that the protein is distributed within cell membrane trafficking compartments and at the very edge of the cell periphery (Fig. 4 *A* and *B*). In contrast, immunocytochemistry of COS7 cells transfected with FAM65B-GFP carrying the mutation of the family showed large puncta in the cytosol, reflecting an accumulation of the protein into dense inclusion bodies and no protein in the membrane (Fig. 4 *C* and *D*).

Knockdown of *fam65b* Causes Hearing Loss in Zebrafish. In situ hybridization in whole-mount zebrafish shows that antisense (Fig. 5*A*) but not sense (Fig. 5*B*) DIG-labeled RNA probes hybridize to *fam65b* mRNA. The purple signals indicate that *fam65b* mRNA expression is detected at the otic vesicle of 3-dpf zebrafish.

To determine the auditory function of *fam65b*, splice site-blocking morpholinos (MO1 and MO2) were used to reduce protein expression (Table S1). MO1 and MO2 retained introns 2 and 3 of *fam65b*, respectively (Fig. 5*C*). Both MO1 and MO2 morphants had fewer saccular hair cells and fewer lateral line neuromasts than control morphants (Fig. 5 *D–H*). No differences in hair cell and neuromast counts were found between MO1 and MO2 morphants. Although MO1 and MO2 morphants showed minor cardiac edema, there was no difference in overall body length among MO1, MO2, and control morphants.

Auditory function of MO1, MO2, and control morphants was assessed at 3 dpf by recording microphonic potentials from hair cells in the otic vesicle. After activation by 200-Hz stimulation, MO1 and MO2 morphants had weaker microphonic response than the controls did (Fig. 5 *I* and *J*). MO1 but not MO2 morphants also had higher microphonic thresholds than controls (Fig. 5*K*). There was no difference in microphonic threshold between MO1 and MO2 morphants.

Discussion

FAM65B (previously called *C6ORF32*, *KIAA0386*, and *PL48*) was first identified in human brain cDNA libraries (18). Naturally occurring mutations of *FAM65B* have not previously been identified in any species. Overexpression of FAM65B in HEK293 and C2C12 cells induces the formation of neurite-like protrusions (19, 20). The protein appears to act on microtubules to form protrusions, because nocodazole, a microtubule-disrupting agent, inhibits FAM65B-induced protrusions. This effect is lost when FAM65B lacks amino acids 56–114 (20) or 173–470 (19). On the other hand, down-regulation of FAM65B causes a decrease in myoblast fusion and differentiation (19). Yeast two-hybrid experiments suggested that FAM65B interacts with NCAM (MIM116930), a membrane-bound glycoprotein that plays a role in cell–cell and cell–matrix adhesion, which is consistent with a role of FAM65B in myoblast fusion (19). In T lymphocytes, FAM65B down-regulates adhesion, polarization, and migration (21). This effect appears to be mediated by inhibition of RHOA (MIM165390), a protein that regulates remodeling of the actin cytoskeleton during cell morphogenesis and hence influences motility. Together, these studies indicate that FAM65B plays a role in regulating cell shape and cell–cell interactions.

In this study, we used a genetic approach to identify FAM65B as a protein required for hearing. Evidence supporting a critical role for FAM65B in hearing includes a mutation coinherited with hearing loss in a large kindred, expression of Fam65b in the cochlea of embryonic and adult mouse, localization of *fam65b* to the zebrafish otic vesicle, and impairment of hearing by gene knockdown in zebrafish. Furthermore, FAM65B localizes to the plasma membrane of the stereocilia hair bundle, the essential cellular organelle in which electrical signals originate and from which they are transmitted after a mechanical stimulus (5). *Fam65b* transcripts are detected early during the development of the cochlea, a stage in which actin-filled microvilli at the apex of hair cells start to rearrange and elongate. Enrichment of Fam65b in the stereocilia of both inner and outer hair cells may suggest that lack of functional Fam65b could hinder the development of the mechanotransduction apparatus. This suggestion is particularly appealing given that stereocilia are filled with cross-linked actin filaments and that FAM65B inhibits RHOA, a protein that regulates the remodeling of cytoskeletal actin (22). Future investigations will help to elucidate the role of FAM65B in the development and operation of the mechanotransduction apparatus of the hair cell.

Materials and Methods

Experimental methods are detailed in *SI Materials and Methods* and include exome sequencing and variant filter strategy, gene expression in mouse inner ear, immunofluorescence in cell monolayers and organotypic cultures, structural modeling of wild-type FAM65B protein, zebrafish knockdown, and hearing evaluation. Fig. S1 shows the specificity of the two antibodies used to detect FAM65B. The nucleotide sequence of all primers and morpholinos utilized in this study are included in Table S1.

ACKNOWLEDGMENTS. We thank Dr. Mary-Claire King from the University of Washington for critical review of the manuscript. This study was supported by National Institutes of Health Grants R01DC009645 (to M.T.), R01DC05575 (to X.Z.L.), and R01GM083897 (to A.F.) and by The Sylvester Braman Family Breast Cancer Institute.

1. Hilgert N, Smith RJ, Van Camp G (2009) Forty-six genes causing nonsyndromic hearing impairment: Which ones should be analyzed in DNA diagnostics? *Mutat Res* 681(2-3): 189–196.
2. Richardson GP, de Monvel JB, Petit C (2011) How the genetics of deafness illuminates auditory physiology. *Annu Rev Physiol* 73:311–334.
3. Rodriguez-Boulan E, Nelson WJ (1989) Morphogenesis of the polarized epithelial cell phenotype. *Science* 245(4919):718–725.
4. Kachar B, Battaglia A, Fex J (1997) Compartmentalized vesicular traffic around the hair cell cuticular plate. *Hear Res* 107(1-2):102–112.
5. Grati M, et al. (2006) Rapid turnover of stereocilia membrane proteins: Evidence from the trafficking and mobility of plasma membrane Ca(2+)-ATPase 2. *J Neurosci* 26(23): 6386–6395.
6. Street VA, McKee-Johnson JW, Fonseca RC, Tempel BL, Noben-Trauth K (1998) Mutations in a plasma membrane Ca^{2+}-ATPase gene cause deafness in deafwaddler mice. *Nat Genet* 19(4):390–394.
7. Schultz JM, et al. (2005) Modification of human hearing loss by plasma-membrane calcium pump PMCA2. *N Engl J Med* 352(15):1557–1564.
8. Wishart MJ, Taylor GS, Dixon JE (2001) Phoxy lipids: Revealing PX domains as phosphoinositide binding modules. *Cell* 105(7):817–820.
9. Habermann B (2004) The BAR-domain family of proteins: A case of bending and binding? *EMBO Rep* 5(3):250–255.
10. Worby CA, Dixon JE (2002) Sorting out the cellular functions of sorting nexins. *Nat Rev Mol Cell Biol* 3(12):919–931.
11. Carlton J, Bujny M, Rutherford A, Cullen P (2005) Sorting nexins—Unifying trends and new perspectives. *Traffic* 6(2):75–82.
12. Carlton JG, Cullen PJ (2005) Sorting nexins. *Curr Biol* 15(20):R819–R820.
13. Cullen PJ, Korswagen HC (2012) Sorting nexins provide diversity for retromer-dependent trafficking events. *Nat Cell Biol* 14(1):29–37.
14. Ellson CD, Andrews S, Stephens LR, Hawkins PT (2002) The PX domain: A new phosphoinositide-binding module. *J Cell Sci* 115(Pt 6):1099–1105.
15. Seet LF, Hong W (2006) The Phox (PX) domain proteins and membrane traffic. *Biochim Biophys Acta* 1761(8):878–896.
16. van Weering JR, Verkade P, Cullen PJ (2010) SNX-BAR proteins in phosphoinositide-mediated, tubular-based endosomal sorting. *Semin Cell Dev Biol* 21(4):371–380.
17. Peter BJ, et al. (2004) BAR domains as sensors of membrane curvature: The amphiphysin BAR structure. *Science* 303(5657):495–499.
18. Nagase T, et al. (1997) Prediction of the coding sequences of unidentified human genes. VII. The complete sequences of 100 new cDNA clones from brain which can code for large proteins in vitro. *DNA Res* 4(2):141–150.
19. Hirayama E, Kim J (2008) Identification and characterization of a novel neural cell adhesion molecule (NCAM)-associated protein from quail myoblasts: Relationship to myotube formation and induction of neurite-like protrusions. *Differentiation* 76(3): 253–266.
20. Yoon S, Molloy MJ, Wu MP, Cowan DB, Gussoni E (2007) C6ORF32 is upregulated during muscle cell differentiation and induces the formation of cellular filopodia. *Dev Biol* 301(1):70–81.
21. Rougerie P, et al. (2013) Fam65b is a new transcriptional target of FOXO1 that regulates RhoA signaling for T lymphocyte migration. *J Immunol* 190(2):748–755.
22. Maekawa M, et al. (1999) Signaling from Rho to the actin cytoskeleton through protein kinases ROCK and LIM-kinase. *Science* 285(5429):895–898.